



KEK Preprint 2000-84  
BELLE-CONF-0015  
August 2000  
H

## CP/T Test with Tau Leptons at Belle

- Examination of T/CP Invariance in

$$e^+e^- \rightarrow \tau^+\tau^- \rightarrow e\mu + \text{neutrinos} \quad -$$

The Belle Collaboration

*Submitted to the XXX<sup>th</sup> International Conference on High Energy Physics,  
July-August 2000, Osaka, Japan.*

**High Energy Accelerator Research Organization (KEK)**

KEK Reports are available from:

Information Resources Division  
High Energy Accelerator Research Organization (KEK)  
1-1 Oho, Tsukuba-shi  
Ibaraki-ken, 305-0801  
JAPAN

Phone: +81-298-64-5137  
Fax: +81-298-64-4604  
E-mail: adm-jouhoushiryou1@ccgemail.kek.jp  
Internet: <http://www.kek.jp>

## CP/T Test with Tau Leptons at Belle

- Examination of T/CP Invariance in

$$e^+e^- \rightarrow \tau^+\tau^- \rightarrow e\mu + \text{neutrinos} -$$

The Belle Collaboration

### Abstract

We have tested T/CP invariance using the CP-odd momentum correlations  $\mathcal{R}$ ,  $\mathcal{A}$  and  $\mathcal{T}_{33}$  in the purely leptonic  $\tau$  reaction,  $e^+e^- \rightarrow \tau^+\tau^- \rightarrow e^\pm/\mu^\mp + (\text{neutrinos})$ , using the first recorded  $4.1 \text{ fb}^{-1}$  of data at KEKB/Belle. Preliminary results indicate that T and CP invariance are valid to within 1% accuracy.

A. Abashian<sup>44</sup>, K. Abe<sup>8</sup>, K. Abe<sup>36</sup>, I. Adachi<sup>8</sup>, Byoung Sup Ahn<sup>14</sup>, H. Aihara<sup>37</sup>, M. Akatsu<sup>19</sup>, G. Alimonti<sup>7</sup>, K. Aoki<sup>8</sup>, K. Asai<sup>20</sup>, M. Asai<sup>9</sup>, Y. Asano<sup>42</sup>, T. Aso<sup>41</sup>, V. Aulchenko<sup>2</sup>, T. Aushev<sup>12</sup>, A. M. Bakich<sup>33</sup>, E. Banas<sup>15</sup>, S. Behari<sup>8</sup>, P. K. Behera<sup>43</sup>, D. Beilene<sup>2</sup>, A. Bondar<sup>2</sup>, A. Bozek<sup>15</sup>, T. E. Browder<sup>7</sup>, B. C. K. Casey<sup>7</sup>, P. Chang<sup>23</sup>, Y. Chao<sup>23</sup>, B. G. Cheon<sup>32</sup>, S.-K. Choi<sup>6</sup>, Y. Choi<sup>32</sup>, Y. Doi<sup>8</sup>, J. Dragic<sup>17</sup>, A. Drutskoy<sup>12</sup>, S. Eidelman<sup>2</sup>, Y. Enari<sup>19</sup>, R. Enomoto<sup>8,10</sup>, C. W. Everton<sup>17</sup>, F. Fang<sup>7</sup>, H. Fujii<sup>8</sup>, K. Fujimoto<sup>19</sup>, Y. Fujita<sup>8</sup>, C. Fukunaga<sup>39</sup>, M. Fukushima<sup>10</sup>, A. Garmash<sup>2,8</sup>, A. Gordon<sup>17</sup>, K. Gotow<sup>44</sup>, H. Guler<sup>7</sup>, R. Guo<sup>21</sup>, J. Haba<sup>8</sup>, T. Haji<sup>4</sup>, H. Hamasaki<sup>8</sup>, K. Hanagaki<sup>29</sup>, F. Handa<sup>36</sup>, K. Hara<sup>27</sup>, T. Hara<sup>27</sup>, T. Haruyama<sup>8</sup>, N. C. Hastings<sup>17</sup>, K. Hayashi<sup>8</sup>, H. Hayashii<sup>20</sup>, M. Hazumi<sup>27</sup>, E. M. Heenan<sup>17</sup>, Y. Higashi<sup>8</sup>, Y. Higashino<sup>19</sup>, I. Higuchi<sup>36</sup>, T. Higuchi<sup>37</sup>, T. Hirai<sup>38</sup>, H. Hirano<sup>40</sup>, M. Hirose<sup>19</sup>, T. Hojo<sup>27</sup>, Y. Hoshi<sup>35</sup>, K. Hoshina<sup>40</sup>, W.-S. Hou<sup>23</sup>, S.-C. Hsu<sup>23</sup>, H.-C. Huang<sup>23</sup>, Y.-C. Huang<sup>21</sup>, S. Ichizawa<sup>38</sup>, Y. Igarashi<sup>8</sup>, T. Iijima<sup>8</sup>, H. Ikeda<sup>8</sup>, K. Ikeda<sup>20</sup>, K. Inami<sup>19</sup>, Y. Inoue<sup>26</sup>, A. Ishikawa<sup>19</sup>, R. Itoh<sup>8</sup>, G. Iwai<sup>25</sup>, M. Iwai<sup>8</sup>, H. Iwasaki<sup>8</sup>, Y. Iwasaki<sup>8</sup>, D. J. Jackson<sup>27</sup>, P. Jalocha<sup>15</sup>, H. K. Jang<sup>31</sup>, M. Jones<sup>7</sup>, R. Kagan<sup>12</sup>, H. Kakuno<sup>38</sup>, J. Kaneko<sup>38</sup>, J. H. Kang<sup>45</sup>, J. S. Kang<sup>14</sup>, P. Kapusta<sup>15</sup>, K. Kasami<sup>8</sup>, N. Katayama<sup>8</sup>, H. Kawai<sup>3</sup>, M. Kawai<sup>8</sup>, N. Kawamura<sup>1</sup>, T. Kawasaki<sup>25</sup>, H. Kichimi<sup>8</sup>, D. W. Kim<sup>32</sup>, Heejong Kim<sup>45</sup>, H. J. Kim<sup>45</sup>, Hyunwoo Kim<sup>14</sup>, S. K. Kim<sup>31</sup>, K. Kinoshita<sup>5</sup>, S. Kobayashi<sup>30</sup>, S. Koike<sup>8</sup>, Y. Kondo<sup>8</sup>, H. Konishi<sup>40</sup>, K. Korotushenko<sup>29</sup>, P. Krokovny<sup>2</sup>, R. Kulasiri<sup>5</sup>, S. Kumar<sup>28</sup>, T. Kuniya<sup>30</sup>, E. Kurihara<sup>3</sup>, A. Kuzmin<sup>2</sup>, Y.-J. Kwon<sup>45</sup>, M. H. Lee<sup>8</sup>, S. H. Lee<sup>31</sup>, C. Leonidopoulos<sup>29</sup>, H.-B. Li<sup>11</sup>, R.-S. Lu<sup>23</sup>, Y. Makida<sup>8</sup>, A. Manabe<sup>8</sup>, D. Marlow<sup>29</sup>, T. Matsubara<sup>37</sup>, T. Matsuda<sup>8</sup>, S. Matsui<sup>19</sup>, S. Matsumoto<sup>4</sup>, T. Matsumoto<sup>19</sup>, K. Misono<sup>19</sup>, K. Miyabayashi<sup>20</sup>, H. Miyake<sup>27</sup>, H. Miyata<sup>25</sup>, L. C. Moffitt<sup>17</sup>, G. R. Moloney<sup>17</sup>, G. F. Moorhead<sup>17</sup>, N. Morgan<sup>44</sup>, S. Mori<sup>42</sup>, T. Mori<sup>4</sup>, A. Murakami<sup>30</sup>, T. Nagamine<sup>36</sup>, Y. Nagasaka<sup>18</sup>, Y. Nagashima<sup>27</sup>, T. Nakadaira<sup>37</sup>, T. Nakamura<sup>38</sup>, E. Nakano<sup>26</sup>, M. Nakao<sup>8</sup>, H. Nakazawa<sup>4</sup>, J. W. Nam<sup>32</sup>, S. Narita<sup>36</sup>, Z. Natkaniec<sup>15</sup>, K. Neichi<sup>35</sup>, S. Nishida<sup>16</sup>, O. Nitoh<sup>40</sup>, S. Noguchi<sup>20</sup>, T. Nozaki<sup>8</sup>, S. Ogawa<sup>34</sup>, R. Ohkubo<sup>8</sup>, T. Ohshima<sup>19</sup>, Y. Ohshima<sup>38</sup>, T. Okabe<sup>19</sup>, T. Okazaki<sup>20</sup>, S. Okuno<sup>13</sup>, S. L. Olsen<sup>7</sup>, W. Ostrowicz<sup>15</sup>, H. Ozaki<sup>8</sup>, P. Pakhlov<sup>12</sup>, H. Palka<sup>15</sup>, C. S. Park<sup>31</sup>, C. W. Park<sup>14</sup>, H. Park<sup>14</sup>, L. S. Peak<sup>33</sup>, M. Peters<sup>7</sup>, L. E. Piilonen<sup>44</sup>, E. Prebys<sup>29</sup>, J. Raaf<sup>5</sup>, J. L. Rodriguez<sup>7</sup>, N. Root<sup>2</sup>, M. Rozanska<sup>15</sup>, K. Rybicki<sup>15</sup>, J. Ryuko<sup>27</sup>, H. Sagawa<sup>8</sup>, Y. Sakai<sup>8</sup>, H. Sakamoto<sup>16</sup>, H. Sakaue<sup>26</sup>, M. Satapathy<sup>43</sup>, N. Sato<sup>8</sup>, A. Satpathy<sup>8,5</sup>, S. Schrenk<sup>44</sup>, S. Semenov<sup>12</sup>, Y. Settai<sup>4</sup>, M. E. Sevior<sup>17</sup>, H. Shibuya<sup>34</sup>, B. Shwartz<sup>2</sup>, A. Sidorov<sup>2</sup>, V. Sidorov<sup>2</sup>, S. Stanić<sup>42</sup>, A. Sugi<sup>19</sup>, A. Sugiyama<sup>19</sup>, K. Sumisawa<sup>27</sup>, T. Sumiyoshi<sup>8</sup>, J. Suzuki<sup>8</sup>, J.-I. Suzuki<sup>8</sup>, K. Suzuki<sup>3</sup>, S. Suzuki<sup>19</sup>, S. Y. Suzuki<sup>8</sup>, S. K. Swain<sup>7</sup>, H. Tajima<sup>37</sup>, T. Takahashi<sup>26</sup>, F. Takasaki<sup>8</sup>, M. Takita<sup>27</sup>, K. Tamai<sup>8</sup>, N. Tamura<sup>25</sup>, J. Tanaka<sup>37</sup>, M. Tanaka<sup>8</sup>, Y. Tanaka<sup>18</sup>, G. N. Taylor<sup>17</sup>, Y. Teramoto<sup>26</sup>, M. Tomoto<sup>19</sup>, T. Tomura<sup>37</sup>, S. N. Tovey<sup>17</sup>, K. Trabelsi<sup>7</sup>, T. Tsuboyama<sup>8</sup>, Y. Tsujita<sup>42</sup>, T. Tsukamoto<sup>8</sup>, T. Tsukamoto<sup>30</sup>, S. Uehara<sup>8</sup>, K. Ueno<sup>23</sup>, N. Ujiie<sup>3</sup>, Y. Unno<sup>3</sup>, S. Uno<sup>8</sup>, Y. Ushiroda<sup>16</sup>, Y. Usov<sup>2</sup>, S. E. Vahsen<sup>29</sup>, G. Varner<sup>7</sup>, K. E. Varvell<sup>33</sup>, C. C. Wang<sup>23</sup>, C. H. Wang<sup>22</sup>, M.-Z. Wang<sup>23</sup>, T.-J. Wang<sup>11</sup>, Y. Watanabe<sup>38</sup>, E. Won<sup>31</sup>, B. D. Yabsley<sup>8</sup>, Y. Yamada<sup>8</sup>, M. Yamaga<sup>36</sup>, A. Yamaguchi<sup>36</sup>, H. Yamaguchi<sup>8</sup>, H. Yamamoto<sup>7</sup>, H. Yamaoka<sup>8</sup>, Y. Yamaoka<sup>8</sup>, Y. Yamashita<sup>24</sup>, M. Yamauchi<sup>8</sup>, S. Yanaka<sup>38</sup>, M. Yokoyama<sup>37</sup>, K. Yoshida<sup>19</sup>, Y. Yusa<sup>36</sup>, H. Yuta<sup>1</sup>, C.-C. Zhang<sup>11</sup>, H. W. Zhao<sup>8</sup>, Y. Zheng<sup>7</sup>, V. Zhilich<sup>2</sup>, and D. Žontar<sup>42</sup>

- <sup>2</sup>Budker Institute of Nuclear Physics, Novosibirsk  
<sup>3</sup>Chiba University, Chiba  
<sup>4</sup>Chuo University, Tokyo  
<sup>5</sup>University of Cincinnati, Cincinnati, OH  
<sup>6</sup>Gyeongsang National University, Chinju  
<sup>7</sup>University of Hawaii, Honolulu HI  
<sup>8</sup>High Energy Accelerator Research Organization (KEK), Tsukuba  
<sup>9</sup>Hiroshima Institute of Technology, Hiroshima  
<sup>10</sup>Institute for Cosmic Ray Research, University of Tokyo, Tokyo  
<sup>11</sup>Institute of High Energy Physics, Chinese Academy of Sciences, Beijing  
<sup>12</sup>Institute for Theoretical and Experimental Physics, Moscow  
<sup>13</sup>Kanagawa University, Yokohama  
<sup>14</sup>Korea University, Seoul  
<sup>15</sup>H. Niewodniczanski Institute of Nuclear Physics, Krakow  
<sup>16</sup>Kyoto University, Kyoto  
<sup>17</sup>University of Melbourne, Victoria  
<sup>18</sup>Nagasaki Institute of Applied Science, Nagasaki  
<sup>19</sup>Nagoya University, Nagoya  
<sup>20</sup>Nara Women's University, Nara  
<sup>21</sup>National Kaohsiung Normal University, Kaohsiung  
<sup>22</sup>National Lien-Ho Institute of Technology, Miao Li  
<sup>23</sup>National Taiwan University, Taipei  
<sup>24</sup>Nihon Dental College, Niigata  
<sup>25</sup>Niigata University, Niigata  
<sup>26</sup>Osaka City University, Osaka  
<sup>27</sup>Osaka University, Osaka  
<sup>28</sup>Panjab University, Chandigarh  
<sup>29</sup>Princeton University, Princeton NJ  
<sup>30</sup>Saga University, Saga  
<sup>31</sup>Seoul National University, Seoul  
<sup>32</sup>Sungkyunkwan University, Suwon  
<sup>33</sup>University of Sydney, Sydney NSW  
<sup>34</sup>Toho University, Funabashi  
<sup>35</sup>Tohoku Gakuin University, Tagajo  
<sup>36</sup>Tohoku University, Sendai  
<sup>37</sup>University of Tokyo, Tokyo  
<sup>38</sup>Tokyo Institute of Technology, Tokyo  
<sup>39</sup>Tokyo Metropolitan University, Tokyo  
<sup>40</sup>Tokyo University of Agriculture and Technology, Tokyo  
<sup>41</sup>Toyama National College of Maritime Technology, Toyama  
<sup>42</sup>University of Tsukuba, Tsukuba  
<sup>43</sup>Utkal University, Bhubaneswer  
<sup>44</sup>Virginia Polytechnic Institute and State University, Blacksburg VA  
<sup>45</sup>Yonsei University, Seoul

## 1. Introduction

It is natural to expect that leptons and quarks have analogous properties in forming the structure of the weak left-handed doublets and right-handed singlets, three generations, and among others, mass hierarchy. There could also be mixing as well as a CP phase between the lepton flavours in the same way as in the quark sector. Even if a leptonic CKM phase exists, the Standard Model (SM) has not shown any detectable amount of CP violation (CPV), compared to that exhibited by K and B mesons, because of a tree diagram predominance in lepton decay. On the other hand, new physics such as multi-Higgs, lepto-quarks and SUSY models are expected to produce appreciable CPV through quantum loop effects and introduce a mass dependence, especially in reactions involving the heaviest lepton, the  $\tau$  [1].

In this work CP-odd momentum correlation observables  $\mathcal{O}$  have been examined in the reaction  $e^+e^- \rightarrow \tau^+\tau^- \rightarrow e^\pm\mu^\mp + (4\nu)$ . CPV could appear at either/both vertices of the  $\tau$ -pair production or/and  $\tau$ -decay so that, without a specific model, the resultant asymmetries of the correlation observables  $\mathcal{O}$  cannot be translated into physical quantities. Although LEP [2] and recently ARGUS [3] reported upper limits on the  $\tau$ 's electric dipole moment assuming that CPV occurs at the production vertex as  $|\text{Re}(d_\tau)/\text{Im}(d_\tau)| < 4.6/1.8 \times 10^{-16}$  e cm and  $|d_\tau| < 1.1 \times 10^{-16}$  e cm, respectively, from the measurements of the correlation observables  $\mathcal{O}$  in the same reaction, we intend first to measure the observables as precisely as possible and then extract an upper limit on  $d_\tau$ .

The CP-odd observables  $\mathcal{O}$  are formed as indicated below in terms of unit momentum-vector correlations between the initial electron  $\hat{q}_-$  and final leptons  $\hat{p}_+$  and  $\hat{p}_-$ , where the lower subscript indicates the lepton charge. The beam axis is taken as the z-axis.

$$\langle \mathcal{A} \rangle \equiv \langle \hat{q}_- \cdot (\hat{p}_+ \times \hat{p}_-) \rangle, \quad (1)$$

$$\langle \mathcal{T}_{33} \rangle \equiv 2 \langle (\hat{p}_+ - \hat{p}_-)_z \cdot \frac{(\hat{p}_+ \times \hat{p}_-)_z}{|\hat{p}_+ \times \hat{p}_-|} \rangle, \quad (2)$$

These quantities are equal to zero when CP/T invariance holds. A double ratio  $\tilde{\mathcal{R}}$ , equivalent to  $\langle \mathcal{A} \rangle$ , is also formed [4] as

$$\begin{aligned} \tilde{\mathcal{R}} &\equiv \mathcal{R}_{\mu^+e^-} \cdot \mathcal{R}_{e^+\mu^-}, \\ &= \frac{N(\mu^+e^-; >)}{N(\mu^+e^-; <)} \times \frac{N(e^+\mu^-; >)}{N(e^+\mu^-; <)}, \\ &= (1 + 2\delta_{\mu^+e^-}) \times (1 + 2\delta_{e^+\mu^-}), \end{aligned} \quad (3)$$

where, for example,  $N(\mu^+e^-; >)$  denotes the detected number of  $\mu^+e^-$  events with  $\mathcal{A} > 0$ . In Eq.(3),  $\delta_{e^+\mu^-}$  and  $\delta_{\mu^+e^-}$  are the T violating portion of the individual samples and they are equivalent to the CP violating portion under CPT invariance,  $\delta = \delta_{e^+\mu^-} = \delta_{\mu^+e^-}$ . Therefore, a non-zero value of the  $\delta$  indicates the existence of CP/T violation and the experimental observable  $\tilde{\mathcal{R}}$  can be expressed as

$$\tilde{\mathcal{R}} = (1 + 4\delta). \quad (4)$$

Furthermore, CPT violation appears as  $\delta_{e^+\mu^-} \neq \delta_{\mu^+e^-}$ .

## 2. The Belle Detector and Event Selection

The Belle detector has been described elsewhere [5]. Among the detector elements, the Central Drift Chamber (CDC) is essential for obtaining unit momentum vectors and the combined information from the Silica Aerogel Cherenkov Counter (ACC), the Time-Of-Flight Counter (TOF), the  $\mu/K_L$  detection system (KLM) and the CsI Electromagnetic Calorimeter (ECL) is used for  $e$  and  $\mu$  identification (ID). For Monte Carlo event generation, KORALB/TAUOLA [6] are used for  $\tau$ -pair production and decays, and AAFHB [7] program is used for two photon samples. Detector simulation is done with a GEANT based program, GSIM, with reconstruction codes written by the Belle collaboration.

Data used in this analysis have been accumulated at the  $\Upsilon(4S)$  energy with an integrated luminosity of  $4.05 \text{ fb}^{-1}$ , corresponding to  $3.7 \times 10^6$   $\tau$ -pairs.

For event selection, each charged track is required to have  $p_t > 0.1 \text{ GeV}/c$  with a primary event vertex of  $|dr| < 1 \text{ cm}$  in the transverse direction and  $|dz| < 5 \text{ cm}$  along the beam, and to point to the detector's barrel region of  $-0.60 < \cos(\theta^{\text{lab}}) < 0.83$ . A photon is a cluster in the ECL with  $E_\gamma > 0.1 \text{ GeV}$ . Using these definitions, two charged tracks with zero net charge and no photons are required. To ensure that the missing momentum flow is due to escaping neutrinos, the polar angle  $\theta_{\text{miss}}$  of the missing momentum vector is required to be in the  $-0.950 < \cos(\theta_{\text{miss}}) < 0.985$ . The two photon  $ee\mu\mu$  events are mostly removed by requiring either a sum of track momenta and photon energies to be  $> 3 \text{ GeV}$  in the c.m. system or one of two tracks have a  $p_t > 1.0 \text{ GeV}/c$ . Radiative Bhabha and  $\mu$ -pairs are further rejected by demanding the sum of track momenta in the c.m. system be  $< 9 \text{ GeV}/c$  and the sum of the ECL energies be  $< 9 \text{ GeV}$ .

While the electron ID is essentially based on the  $E^{\text{lab}}/p^{\text{lab}}$  ratio and the muon ID uses the particle range in KLM,  $e/\mu/\pi$  probabilities comprising information from ACC, TOF, KLM, ECL and  $dE/dx$  in the CDC are calculated for each track. An electron should satisfy the requirements:  $E^{\text{lab}}/p^{\text{lab}} > 0.8$ , the combined e-probability (eid-prob)  $> 0.6$ , and momentum  $p^{\text{lab}} > 0.5 \text{ GeV}/c$ ; a muon should satisfy a certain class of KLM range requirements and  $p^{\text{lab}} > 1.2 \text{ GeV}/c$ ; a pion has eid-prob  $< 0.10$  with  $p^{\text{lab}} > 1.2 \text{ GeV}/c$  and must not have a range in the KLM that is characteristic of a  $\mu$ . Particle identification (PID) efficiencies for  $e$  and  $\mu$  are evaluated as 86.4% and 91.5%, respectively, with fake rates of 0.08% and 1.5%.

The event selection rate is evaluated by MC: The main background arises from the two photon processes and  $\pi$  misidentification as  $\mu$  or  $\tau \rightarrow \pi\nu$ , which amount to 3.0% and 1.6%, respectively. Other contributions can be neglected. The expected signal rate is  $7.5 \times 10^3$  events per  $1 \text{ fb}^{-1}$ .

## 3. Analysis

The resulting data sample contains  $31.8 \times 10^3$  events, and is summarized in Table 1. The distributions of  $\cos(\theta^{\text{lab}})$ ,  $\phi$ -angle and momentum  $p^{\text{lab}}$  for  $e$  and  $\mu$  are shown in Fig.1 together with their ratios between respective leptons of the negative and positive charge.

Stable constant ratios of 1.0 are found for all distributions, except for  $\cos(\theta^{\text{lab}})$  of  $e^\pm$ . The deviation from unity in both large electron  $\cos(\theta^{\text{lab}})$  regions is due to the asymmetric two-photon  $ee\mu\mu$  contribution mentioned below. All of the observed ratios, including that for the electron  $\cos(\theta^{\text{lab}})$  distribution, agree with MC predictions and no charge dependent detection efficiency is seen. While the distributions generally agree well with MC, some disagreement is found, particularly in the momentum distribution for electrons, which indicates that our simulation program is not yet completed. Therefore, we would now like to rely on data to demonstrate our understanding of the system rather than on MC simulation.

Distributions of the observables  $\mathcal{A}$  and  $\mathcal{T}_{33}$  are shown in Fig.2 and their corresponding means together with  $\mathcal{R}$  are listed in Table 2. In order to examine possible local detector defects, the detector system is segmented into octants in the  $\phi$ -angle and the stability of  $\tilde{\mathcal{R}}$  distributions is analyzed by fixing either  $e$  or  $\mu$  in each octant. No appreciable peculiarity is detected, as shown in Fig.3. Run-dependent data quality is also tested by examining the  $\tilde{\mathcal{R}}$  stability over 19 segments of the full data. The run dependence of the  $\tilde{\mathcal{R}}$  distribution is found to be consistent within the statistical errors.

Contributions to the observables from particle misidentification and  $ee\mu\mu$  contamination are estimated using the method discussed in Ref.[4]. As long as  $\mathcal{R} \approx 1$  or  $< \mathcal{A}(\mathcal{T}_{33}) > \ll 1$ , the true values  $\mathcal{O}^{\text{true}}$  can be expressed in the following form:  $\mathcal{O}^{\text{true}} = \mathcal{O}^{\text{obs}}(1 - \zeta_{\mathcal{O}}/\mathcal{O}^{\text{obs}})$ ;  $\zeta_{\mathcal{O}} = \alpha_{\text{BG}} \cdot (\mathcal{O}^{\text{BG}} - \mathcal{O}^{\text{obs}})$ , where  $\alpha$  is the contamination fraction in the signal samples,  $\mathcal{O}^{\text{obs}}$  is the observed value for the relevant quantity and  $\zeta_{\mathcal{O}}$  is a correction term.

The  $\pi$  contamination rate due to wrong PID as  $\mu$  predominates  $\alpha_{\text{PID}}$  as  $(2 \pm 1)\%$ , since wrong  $e$ -PID rate can be disregarded.  $\mathcal{O}^{\text{BG}}$  due to the wrong PID is obtained using the remaining tracks as non- $\mu$  particles which passed all kinematical criteria with an  $e^+/e^-$  partner as listed in Table 2.

For the effect of the  $ee\mu\mu$  contamination the same sign combination of  $e^\pm\mu^\pm$  is analyzed by applying the same selection criteria except for the charges and their resulting rates are multiplied by the MC deduced ratio between the opposite and same sign samples to estimate  $e^\pm\mu^\mp$  rates, as found in Table 2. The obtained  $\alpha_{\gamma\gamma}$  is  $(2.8 \pm 0.3)\%$ .

Because of the small contamination rates,  $\zeta_s$  do not produce significant contributions as shown in Table 1. Using these numbers we extract the background subtracted  $\mathcal{O}$  values separately for  $e^+\mu^-$  and  $\mu^+e^-$ .

KEKB is an energy-asymmetric collider with a beam crossing angle of 22 mrad, so that

the system is not symmetric with respect to the forward/backward (F/B) directions and azimuthal ( $\phi$ ) rotation. Furthermore, although the Z-boson also contributes only weakly, the system is intrinsically asymmetric with respect to negative/positive charges ( $-/+$ ). For two-photon processes such as  $e\mu\mu$  and  $e\pi\pi$ , the kinematical criteria do not function equally well for  $e^+$  or  $e^-$  modes due to the asymmetric boost of the system. For this reason,  $e^+\mu^-$  ( $e^+X^-$ ) has a somewhat larger rate than  $\mu^+e^-$  ( $X^+e^-$ ), see the second and third columns of Table 1.

However, our observables  $\mathcal{O}$  are in principle CP symmetric. They depend on the z-component of the vector product between a positive and negative charged particle,  $(\hat{p}_+ \times \hat{p}_-)_z$ , which means that their relative x and y components are essential but not their z components. Thus, F/B and  $-/+$  asymmetries do not matter. Furthermore, the integration over the  $\phi$ -angle diminishes the effects of any  $\phi$  rotation asymmetry.

In order to examine a possible systematic offset of the observables, we form our observables  $\mathcal{O}$  using high multiplicity samples such as from  $B\bar{B}$  and continuum events which do not have any angular correlations. The obtained  $\mathcal{O}_{\text{mul}}$ s are listed in Table 2 and taken as the offset of the detector system on the background-subtracted  $\mathcal{O}^{\text{obs}}$ s. It is also possible to detect the above systematic offset behavior in deviations of the CP conserving  $\mathcal{O}^{\text{obs}}$  values in Table 2.

The resulting final asymmetries are obtained by adding the two background-subtracted  $\mathcal{O}^{\text{obs}}$ s of opposite charge combination modes and subtracting the offset  $\mathcal{O}_{\text{mul}}$ s for the individual observables as,

$$\delta = -0.010 \pm 0.006 \pm 0.002, \quad (5)$$

$$\langle \mathcal{A} \rangle = (3.2 \pm 1.8 \pm 0.5) \times 10^{-3}, \quad (6)$$

and

$$\langle \mathcal{T}_{33} \rangle = (-6.8 \pm 5.3 \pm 0.9) \times 10^{-3}, \quad (7)$$

where the first errors are statistical and the second errors are systematic ambiguities arising from the background subtraction and the offset estimate for the detector system.

#### 4. Results

We have measured CP violation observables  $\mathcal{O}$  in the reaction  $e^+e^- \rightarrow \tau^+\tau^-$  where  $\tau \rightarrow e/\mu\nu\bar{\nu}$ , using the first 4.1 fb $^{-1}$  data recorded at KEKB/Belle. The resulting values of  $\mathcal{O}$  are consistent with CP invariance within experimental errors, and their 90% CL upper limits are set as

$$|\delta| < 0.018, \quad (8)$$

$$|\langle \mathcal{A} \rangle| < 0.0055, \quad (9)$$

$$|\langle \mathcal{T}_{33} \rangle| < 0.014. \quad (10)$$

Without assuming CPT invariance, we obtain  $\delta_{e^+\mu^-} = -0.006 \pm 0.008 \pm 0.004$  and  $\delta_{\mu^+e^-} = -0.014 \pm 0.008 \pm 0.003$  from the individual  $\mathcal{R}$ -ratios in  $e^+\mu^-$  and  $\mu^+e^-$  modes

respectively. T invariance is then verified to be valid within the experimental errors of about 1% accuracy in the purely leptonic reactions. The agreement between two  $\delta_{e^+\mu^-}$ s indicates that CP invariance holds also at the same accuracy.

We are working on the translation of these results into physical quantities such as the  $\tau$  electric dipole moment by introducing such effects into KORALB.

#### Acknowledgements

We gratefully acknowledge the efforts of the KEKB group in providing us with excellent luminosity and running conditions and the help with our computing and network systems provided by members of the KEK computing research center. We thank the staffs of KEK and collaborating institutions for their contributions to this work, and acknowledge support from the Ministry of Education, Science, Sports and Culture of Japan and the Japan Society for the Promotion of Science; the Australian Research Council and the Australian Department of Industry, Science and Resources; the Department of Science and Technology of India; the BK21 program of the Ministry of Education of Korea and the Basic Science program of the Korea Science and Engineering Foundation; the Polish State Committee for Scientific Research under contract No.2P03B 17017; the Ministry of Science and Technology of Russian Federation; the National Science Council and the Ministry of Education of Taiwan; the Japan-Taiwan Cooperative Program of the Interchange Association; and the U.S. Department of Energy.

## REFERENCES

- [1] N. Wermes, Nucl. Phys. B (Proc. Suppl.) **55C** (1997) 313.  
 [2] L3 Collaboration, Phys. Lett. **B434** (1998) 169;  
 OPAL Collaboration, Phys. Lett. **B431** (1998) 188.  
 [3] H. Albrecht et al. (ARGUS Collaboration), hep-ex/0004031.  
 [4] T. Ohshima et al., Prog. Theor. Phys., **99** (1998) 413.  
 [5] CDC: H. Hirano et al., KEK Preprint 2000-2. to be published in Nucl. Instr. Meth.; ECL: H. Ikeda et al., Nucl. Instr. Meth. **441** (2000) 401;  
 KEKB B-Factory Design Report, KEK Report 95-7 (1995).  
 [6] KORALB(v.2.4)/TAUOLA(v.2.6): S. Jadach and Z. Was, Comp. Phys. Commun. **85** (1995) 453 and *ibid*, **64** (1991) 267, *ibid*, **36** (1985) 191; S. Jadach, Z. Was, R. Decker and J.H. Kühn, Comp. Phys. Commun. **64** (1991) 275, *ibid*, **70** (1992) 69, *ibid*, **76** (1993) 361.  
 [7] AAFH: F. A. Berends, P. H. Daverveldt, R. Kleiss, Comp. Phys. Commun. **40** (1986) 285.

Table 1: The correction factor  $\zeta$  arising from the wrong PID and two-photon  $ee\mu\mu$  contamination is listed for three observables. See the text for the definition of  $\zeta$ .

	mode	observed ev.	$\zeta_{\mathcal{R}}$	$\zeta_{\langle A \rangle}$	$\zeta_{\langle T_{33} \rangle}$
signal	$e^+\mu^-$	15,781			
	$\mu^+e^-$	16,079			
wrong PID	$e^+X^-$	22,222	$(0.14 \pm 0.08) \times 10^{-2}$	$-(0.56 \pm 0.66) \times 10^{-4}$	$(0.57 \pm 1.84) \times 10^{-4}$
	$X^+e^-$	23,530	$(0.19 \pm 0.10) \times 10^{-2}$	$(0.86 \pm 1.69) \times 10^{-4}$	$(2.51 \pm 3.46) \times 10^{-4}$
$\gamma\gamma$	$e^+\mu^-$	$446 \pm 59$ ‡	$(0.77 \pm 0.41) \times 10^{-2}$	$-(0.82 \pm 51.55) \times 10^{-4}$	$(4.96 \pm 13.80) \times 10^{-4}$
	$\mu^+e^-$	$462 \pm 51$ ‡	$(0.09 \pm 0.46) \times 10^{-2}$	$-(5.74 \pm 8.00) \times 10^{-4}$	$(0.21 \pm 7.95) \times 10^{-4}$
multi- hadrons	$X^+Y^-$	2.3 M			

‡ The observed numbers of the same sign  $e^\pm\mu^\mp$  samples are normalized using a MC based ratio between the wrong and same sign samples for the  $ee\mu\mu$  reaction. The recorded 4.05 fb<sup>-1</sup> of data are used in this analysis.

Table 2: Three different CP-odd observables are listed in the large second column for  $e^+\mu^-$  and  $\mu^+e^-$  mode, respectively. Asymmetries for background and normalization processes are given in the 2nd, 3rd, and 4th columns, respectively; see the text for details. The indicated errors are statistical only.

	mode	$\mathcal{R}^{\text{obs}}$	$\langle A \rangle^{\text{obs}}$	$\langle T_{33} \rangle^{\text{obs}}$
signal	$e^+\mu^-$	$1.028 \pm 0.016$	$0.0078 \pm 0.0025$	$-0.0064 \pm 0.0074$
	$\mu^+e^-$	$1.006 \pm 0.016$	$0.0028 \pm 0.0025$	$-0.0059 \pm 0.0074$
wrong PID	$e^+X^-$	$1.105 \pm 0.013$	$0.0058 \pm 0.0012$	$-0.0043 \pm 0.0034$
	$X^+e^-$	$1.109 \pm 0.013$	$0.0058 \pm 0.0012$	$0.0029 \pm 0.0032$
$\gamma\gamma$	$e^+\mu^-$	$1.40 \pm 0.26$	$0.0049 \pm 0.0184$	$0.0112 \pm 0.0423$
	$\mu^+e^-$	$1.04 \pm 0.17$	$-0.0171 \pm 0.0155$	$-0.0066 \pm 0.0264$
multi- hadrons	$X^+Y^-$	$1.031 \pm 0.001$	$0.0024 \pm 0.0004$	$0.0003 \pm 0.0005$

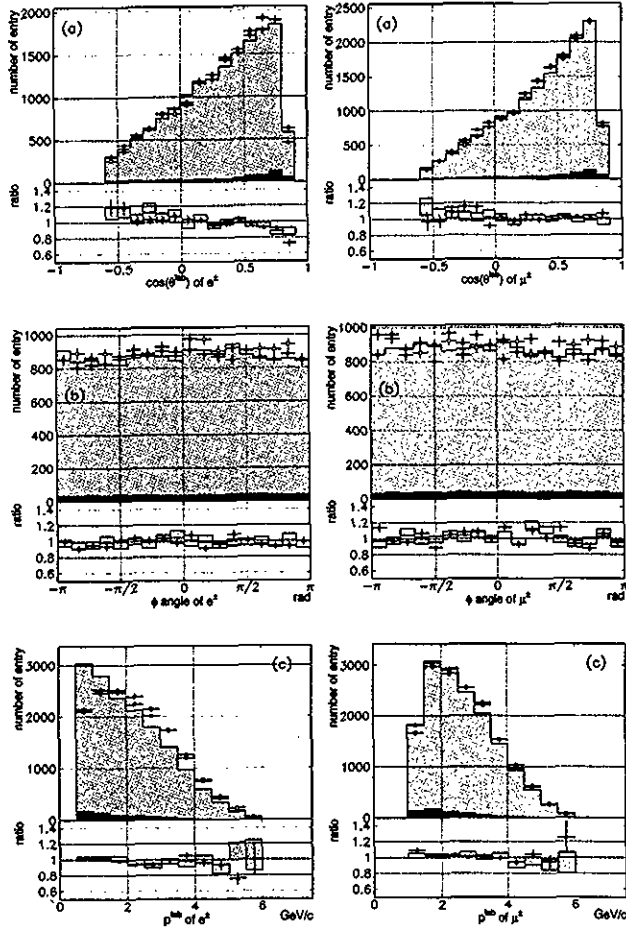


FIG. 1. Distributions of (a)  $\cos(\theta^{\text{lab}})$  (b)  $\phi$ -angle and (c)  $p^{\text{lab}}$  for  $e^\pm$  (left) and  $\mu^\pm$  (right). Data for positive and negative charged particles are plotted by closed and open circles respectively; MC distributions for either charged particle are shown by the shaded (yellow) histogram; and the contamination from wrong PID and two-photon  $ee\mu\mu$  are by the darker (red and blue) histograms. The number of generated MC events is normalized to the recorded total integrated luminosity. The ratios between the distributions for the opposite charged samples are also plotted for the data (closed circles) and MC simulation (shaded (yellow) histograms).

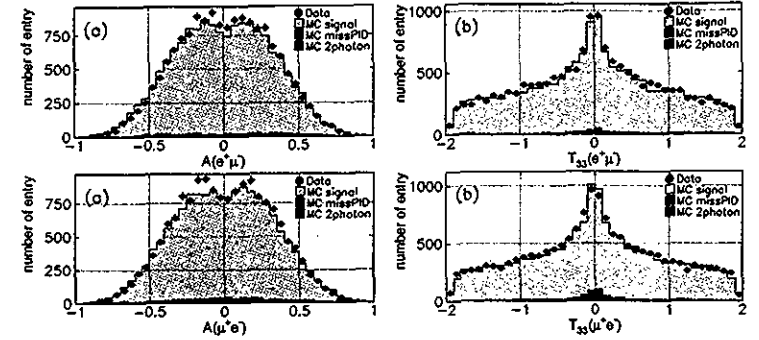


FIG. 2. The observed  $A$  and  $T_{33}$  distributions are plotted in (a) and (b) for  $e^+\mu^-$  (each upper Figure) and  $\mu^+e^-$  (each lower Figure) modes, respectively. Data are indicated by closed circles, the MC simulation result by the shaded (yellow) histogram, and the contamination from wrong PID and two-photon  $ee\mu\mu$  by darker (red and blue) histograms.

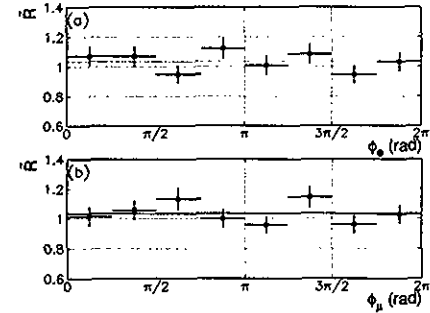


FIG. 3. The  $\phi$  distributions for the observable  $\tilde{\mathcal{R}}$ .  $\tilde{\mathcal{R}}$  is segmented by referring  $\phi$ -angle of  $e^\pm$  in (a) and  $\mu^\pm$  in (b).